

Curvature Driven Transport of Mouse Macrophages in a Pulsating Magnetic Garnet Film Ratchet

Prajnaparamita Dhar,[†] Pietro Tierno,^{‡,§} Joan Hare,[§] Tom H. Johansen,^{||} and Thomas M. Fischer^{*,†,⊥}

Department of Chemistry and Biochemistry, The Florida State University, Tallahassee, Florida 32306, Departament de Química Física, Universitat de Barcelona, Martí i Franquès 1, E-08028 Barcelona, Spain, Institute of Molecular Biophysics, The Florida State University, Tallahassee, Florida 32304, Department of Physics, University of Oslo, Blindern, Norway, and Physikalisches Institut für Experimentalphysik V, Universität Bayreuth, 95440 Bayreuth

Received: August 10, 2007; In Final Form: September 5, 2007

Magnetic fields varying on the colloidal length scale are used for the directed transport of magnetically labeled biological cells. The transport is achieved by using the ratchet effect which relies on an asymmetric, symmetry broken periodic potential where nonequilibrium fluctuations or oscillations generate a net cell current. Ferrofluid ingested mouse macrophages were placed on a magnetic garnet film with alternating stripe domain patterns, and a pulsating magnetic potential is provided by superposing an oscillating magnetic field normal to the film. The symmetry of the resulting periodic stripe potential is broken locally by the curvature of the stripes. We show, both experimentally and theoretically, the curvature of such stripes required for inducing directed transport of the macrophages in the ratchet. This may be useful for microfluidic devices such as a digital colloidal shift register for magnetically labeled biological cells.

Introduction

The variety of chemical and biological functionalities of colloidal particle surfaces makes them important tools in the medical, biochemical, and biophysical fields. Colloidal particles are used for novel forms of DNA sequencing¹ and optical barcoding,² as carriers of biomolecules and proteins in microfluidic channels,³ and as fluorescent markers in microrheological experiments of the cytoskeleton.^{4–9} Magnetic manipulation of paramagnetic colloidal particles and ferrofluids is used extensively in medicine and in developing microfluidic devices for biomedical analysis. Various biological cells like the Jurkat cells were separated from the blood using CD3 coated magnetic particles by trapping them in a microchannel.¹⁰ Magnetic *E. coli* cells attached to 2.8 μm Dynabeads were captured and isolated from blood samples on a microdevice using an external magnetic field¹¹. Magnetic colloidal particles are also used in the hyperthermia treatment of cancer,^{12–15} in which magnetic field gradients are first used to collect and enrich these particles in the cancerous part of the human body and then destroy the cancerous tissue using high-frequency magnetic fields that heat the particles and thus the tissue. Important issues such as the compatibility and nontoxicity of these particles¹⁶ in the human body have been addressed extensively, and they can be used directly when manipulating the same kind of particles in vitro on microfluidic devices that analyze or detect specific chemical or biological species. Magnetic manipulation of colloidal particles in the human body is limited to fields with spatial variations on the macroscopic scale. These limitations, however,

do not exist on a lab-on-a-chip device, where magnetic fields can be created that vary on the colloidal length scale. For example, Yellen et al.^{17,18} use lithographic deposition of cobalt to form ferromagnetic micro-patterns. Gunnarson et al.¹⁹ deposited a permalloy into elliptic island patterns and showed the ability to transport paramagnetic particles along the ellipses. We use ferrimagnetic ferrite garnet films to produce the magnetic heterogeneities. These heterogeneities are self-assembled magnetic domain patterns that can be altered in shape and size with external homogeneous magnetic fields. Applying an external field modulation renders the magnetic field heterogeneities time dependent, and the magnetic particles are in a nonequilibrium environment.

Here, we explore the use of magnetic fields varying on the colloidal length scale for achieving directed transport in magnetically labeled biological cells. The transport was achieved by using the ratchet effect²⁰ which relies on an asymmetric, symmetry broken periodic potential where nonequilibrium fluctuations or oscillations generate a net current. Ferrofluid ingested mouse macrophages were placed on a magnetic garnet film with alternating stripe domain patterns, and the pulsating potential was provided by superposing an oscillating magnetic field normal to the film. The symmetry of the resulting periodic stripe potential is broken locally by the curvature of the stripes. We show, both experimentally and theoretically, the curvature of such stripes required for inducing directed transport of the macrophages in the ratchet. This may be useful for microfluidic devices such as a digital colloidal shift register for magnetically labeled biological cells.

Materials and Methods

Macrophages. Pixie H32.12 mouse macrophages obtained from American Type Culture Collection (ATCC) were cultured in Joklik's minimum essential medium (JMEM, Sigma, enriched with 10% heat inactivated fetal calf serum (Harlan), 1%

* Corresponding author.

[†] Department of Chemistry and Biochemistry, The Florida State University.

[‡] Universitat de Barcelona.

[§] Institute of Molecular Biophysics, The Florida State University.

^{||} University of Oslo.

[⊥] Universität Bayreuth.

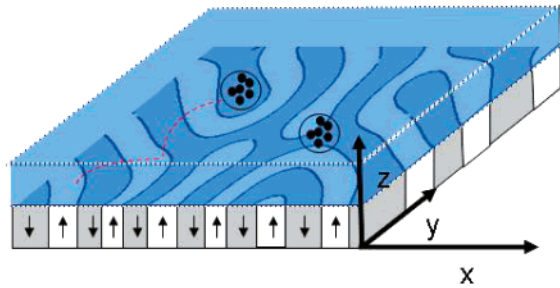


Figure 1. Scheme of a magnetic garnet film with alternating magnetized stripe domains. Cells doped with paramagnetic particles are immersed in an aqueous solution above the film and are transported perpendicular to the stripe pattern when the film is modulated with an oscillating external magnetic field normal to the garnet film.

penicillin G/streptomycin/amphotericin B of $100\times$ mix (Hy-Clone) and $10\text{ }\mu\text{g/mL}$ gentamicin) in a humidified $37\text{ }^{\circ}\text{C}$ incubator with 5% CO_2 . $100\text{ }\mu\text{L}$ ferrofluid containing $5\text{--}50\text{ nm}$ sized Fe particles were added with 2 mL of cells (cell density of $9.5 \times 10^5\text{ cells/mL}$) and placed in a Petri dish. After 24 h , 90% of the cells were found to have adhered to the dish, and the magnetic particles had been phagocytized. The cells were mechanically detached from the surface by repeated forceful expulsion of media at a 45° angle to the plate surface with a narrow-tip transfer pipet.

Magnetic Garnet Film. The cells under observation are placed on a $4\text{ }\mu\text{m}$ magnetic garnet film of composition $\text{Y}_{2.5}\text{Bi}_{0.5}\text{Fe}_{5-q}\text{Ga}_q\text{O}_{12}$ ($q = 0.5\text{--}1$).²¹ To prevent the cells from sticking to the surface, the garnet film was coated with polysodium 4-styrene sulfonate. The magnetic garnet film of spontaneous magnetization ($M_s = 11\text{ kA/m}$) has domains forming stripes alternating between up and down magnetization with a typical wavelength of $12\text{ }\mu\text{m}$ (about the size of the macrophages, Figure 1). Manipulation of the stripe pattern using alternating magnetic fields in the kHz region allows changing the curvature of the stripes. The domain stripes give rise to a symmetric and periodic magnetic potential which can be varied by the application of an external magnetic field perpendicular to the film. The width of the domain with magnetization parallel to the external field grows at the expense of the domain with the antiparallel magnetization.

The gravity and the electrostatics are efficiently able to confine the cells at a plane a few nanometers above the surface of the garnet film. The cells along with the stripe pattern were observed using a polarization microscope (Leica, DMLP). The stripe pattern could be visualized because of the polar Faraday effect. The external magnetic field was provided by a coil placed under the garnet film. The modulations in the field were achieved by connecting the coil to an amplifier being fed by a wave generator. The motion of the cells was followed by using a color camera and videos were recorded at 25 fps .

Results and Discussions

Application of a magnetic field normal to the garnet film changes the domain structure and hence the interaction with the ferrofluids ingested macrophages. In the absence of an external field, the domains with downward magnetization have the same width as the domains with upward magnetization, and the field above both domains is similar in strength but opposite in orientation. The strongest magnetic field is above the domain walls where it increases logarithmically on approaching the domain walls. The ingested ferrofluid and thus the macrophages are attracted to the position of the strongest field, and in zero external field, we find them located right above one of the

domain walls (Figure 2 top and bottom; $t = 0\text{ s}$). An external field normal to the garnet film increases the size of the domain having a magnetization parallel to the external field and decreases the size of the antiparallel domain. As a consequence, the magnetic field strength above the majority domain increases at the expense of the minority domain, and the macrophages move from the region above the domain wall to the interior of the majority domain (Figures 2, $t = 0.084\text{ s}$). Figure 2 top and bottom shows the motion of a macrophage above the stripe pattern that occurs during one cycle ($f = 3\text{ Hz}$) of the external magnetic field. Both macrophages move from above the domain wall ($t = 0\text{ s}$) to the upward magnetized majority domain interior (bright stripe $t = 0.084\text{ s}$), back to a domain wall ($t = 0.168\text{ s}$), in the downward magnetized majority domain interior (dark stripe $t = 0.252\text{ s}$) and then back to a domain wall ($t = 0.336\text{ s}$). Figure 2 (top) shows a macrophage above a region with a straight stripe pattern, while Figure 2 (bottom) shows a macrophage above a curved $\kappa \approx 0.085\text{ }\mu\text{m}^{-1}$ pattern. The motion of both macrophages is different in the sense that the macrophage above the straight pattern tends to return to the original domain wall when the external field normal to the film returns to zero, while the macrophage above the curved stripes proceeds to the next domain wall located at the concave side. The consequence of this different behavior is that macrophages above a straight domain pattern tend to stay near the domain wall where they have been attached before the application of the external field. The macrophages above the curved domain pattern, however, proceed by one wavelength $\lambda = 12\text{ }\mu\text{m}$ in the concave direction of the stripe pattern during each cycle. Hence, we have a net motion of the macrophages with speed $v = \lambda f$ that only occurs above the regions where the stripe pattern changes direction. Figure 3 shows the motion of the macrophages on a larger time scale after 1, 2, 3, 4, and 5 cycles. While the macrophage in Figure 3 (top) above the straight stripes remains at its location, the one above the curved stripes in Figure 3 (bottom) proceeds by $5\lambda = 60\text{ }\mu\text{m}$.

In Figure 4, we summarize our observations obtained from 56 macrophages above stripes of different curvature by plotting the probability p of the macrophages to move in the concave direction versus the normalized curvature $\kappa\lambda$. Macrophages rarely move above stripes of curvature below $\kappa\lambda < 0.5$. Above a curvature of $\kappa\lambda > 0.5$, they seem to respond with a directed motion almost deterministically. It is therefore clear that one may use the curvature of the stripe pattern to guide the macrophages along a predetermined path on top of the film. The motion is stepwise with an exact progression of $1\text{ }\lambda/\text{cycle}$ such that one does not lose information of the whereabouts of each macrophage. This might be useful when dealing with a large amount of individual cells above the film.

Simulation of the Ratchet Potential.

We model the motion of the macrophage by an overdamped Langevin equation across a cylindrical symmetric (coordinates r, z, φ) stripe pattern of the film:

$$\nabla U(r, z, t) = -\eta \dot{\mathbf{x}} + \mathbf{F}_{\text{random}}$$

with a magnetic potential

$$U(r, z, t) = -\mu_0 \chi_{\text{eff}} V \mathbf{H}(r, z, t)^2$$

that is proportional to the square of the magnetic field, the effective susceptibility $\chi_{\text{eff}} = 0.8$, and volume $V \approx 2.7 \times 10^{-15}\text{ m}^3$ of the ingested ferrofluids and a fluctuating random force

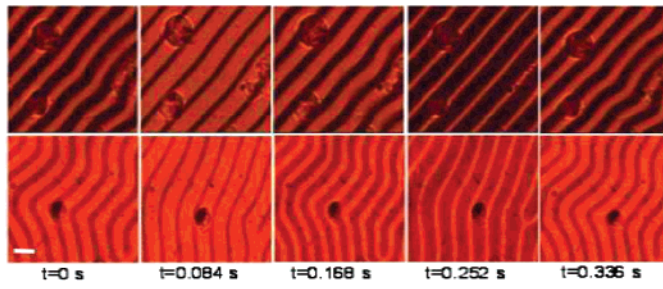


Figure 2. Polarization microscope images of a macrophage with phagocitized ferrofluid above the garnet film. The domain structure of the magnetic field is visualized making use of the polar Faraday effect. The sequence of images shows the motion of the macrophage above a straight (top) and above a curved (bottom) stripe domain pattern of the garnet film during one modulation period $T = 0.336$ s. The modulation voltage was 5 V. A movie of the motion can be viewed in the Supporting Information. The right scheme shows the motion of the domains and the phages for a straight and curved stripe pattern.

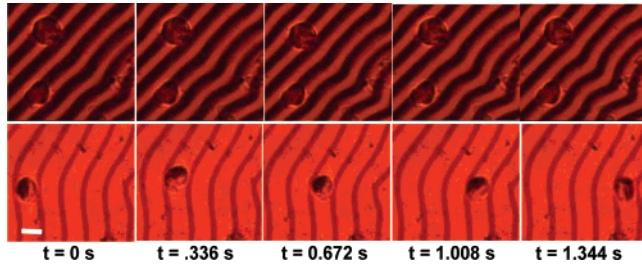


Figure 3. Polarization microscope images of a macrophage with phagocitized ferrofluid above the garnet film. The sequence of images shows the motion of the macrophage above a straight (top) and above a curved (bottom) stripe domain pattern of the garnet film during 5 cycles. Conditions are the same as in Figure 2.

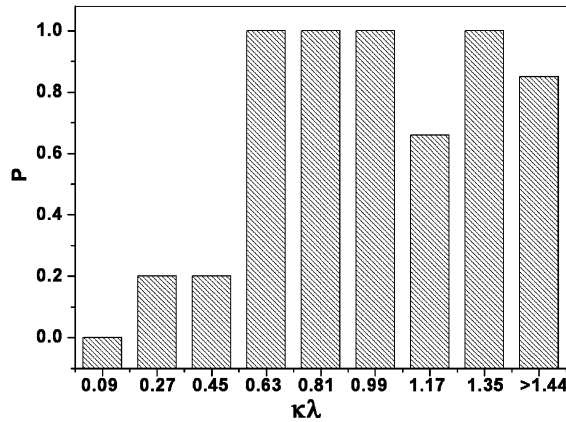


Figure 4. Experimentally determined probability of hopping in the direction of the stripe curvature after one cycle, plotted as a function of the normalized stripe curvature.

F_{random}. The magnetic field of the cylindrical stripe pattern of wave length λ can be written as a sum of the magnetic fields $\mathbf{H} = \sum_m \pm \mathbf{H}_{m,\pm}$ from magnetic bubble domains of radius $R_{m\pm} = (m + 1/2)\lambda \pm (\lambda - d)/2$, $m = 0, 1, 2, \dots$ that are modulated in width as a function of time according to $d = \lambda/2 + \delta \sin \omega t$. The magnetic field of a single bubble $\mathbf{H}_{m,\pm}$ is given by: where $Q_{1/2}$ is a Legendre function of the second kind, Π is the complete elliptic integral of the third kind, and $H_{\text{ex}} = M\delta/2\lambda$

$$\frac{H_{m\pm,r}}{M} = \mp \sqrt{\frac{R_{m\pm}}{r}} Q_{1/2} \left(\frac{r^2 + R_{m\pm}^2 + z^2}{2rR_{m\pm}} \right)$$

$$k_{m\pm} = \sqrt{\frac{4rR_{m\pm}}{z^2 + (r + R_{m\pm})^2}}, n_{\pm} = \frac{2r}{r \pm \sqrt{r^2 + z^2}}$$

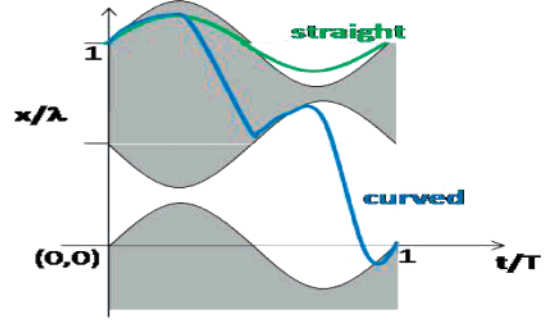


Figure 5. Contour plot of the magnetostatic potential of a concentric modulated $H_{\text{ex}}/M = 0.6$ stripe pattern as a function of the radial position and as a function of time. The blue lines show the position of the local energy minima as a function of time.

$$\frac{H_{m\pm,z}}{M} = \pm \frac{2}{\pi} \left(\frac{\sqrt{r^2 + z^2} - R_{m\pm}(\sqrt{r^2 + z^2} - r)\Pi(n_{\pm}, k_{m\pm})}{z\sqrt{(r + R_{m\pm})^2 + z^2}} + \frac{(\sqrt{r^2 + z^2} + R_{m\pm})(\sqrt{r^2 + z^2} + r)\Pi(n_{\pm}, k_{m\pm})}{z\sqrt{(r + R_{m\pm})^2 + z^2}} \right)$$

$\sin \omega t$ is the external magnetic field. In Figure 5, we show a plot of the potential as a function of the radius r and time t for an elevation of the ferrofluids of $z = 1.4 \mu\text{m}$. The periodic modulation leads to a periodic change of the position of the energy minima above the film. At zero external fields, we find the energy minima above the domain walls. When the external field is applied, the minimum continuously oscillates around the domain wall position at the larger radii $r/2\lambda > 4$ (blue lines). The changes in the energy minimum position with time become more pronounced at the smaller radii $r/2\lambda < 4$ explaining why the macrophages are more susceptible to hop at the strongly curved domain walls. The direction of the hopping however cannot be explained by the potential only. As is inherent to the nature of the ratchet, the direction of motion is a complicated function of the noise level in the system. The curvature of the stripe domain pattern breaks the symmetry of the magnetic potential, and hence, the generic situation is a net current pointing in or opposite to the direction of curvature. In our experimental case, this direction is in the direction of the curvature.

Conclusions

In the present paper, we have shown the successful transportation of magnetically doped biological cells in a precise manner where one is able to predict the location of the cells at each instant. We achieve this by magnetic manipulation of the cells without involving strong magnetic fields but instead using strong magnetic field gradients. This prevents the cell not just from getting lost but also from losing identity which is a common problem for most other magnetic transport mechanisms. This method can especially be useful for single cell assay in lab-on-a-chip studies as well as for studies where the desire is to track the cells while moving them around. Our work also demonstrates the theory of the movement of magnet particle-containing cells within a magnetic field. Drug delivery using ferrofluids is becoming a common technique,²² and our method may be able to aid in studies relating to the efficiency of this technique. A particular feature of noise driven ratchets is the current inversion upon moderate changes of the ratchet parameters. This should enable the efficient separation of cells. The description should help others understand cellular movements in this process as well as novel in vitro situations.

Acknowledgment. We thank Ramanathan Murganathan for providing us with ferrofluid. We thank Donny Magana and Geffory Strouse for the SQUID measurements. This material is based upon work supported by the National Science Foundation under CHE-0649427. T.H.J. thanks The Research Council of Norway for financial support.

Supporting Information Available: Movie clip of a macrophage with phagocitized ferrofluid moving across the stripe pattern above the garnet film. The magnetic modulation of the film lets the macrophage move along the path of maximum curvature of the stripe pattern. This material is available free of charge via the Internet at <http://pubs.acs.org>.

References and Notes

- (1) Seeger, S.; Monajembashi, S.; Hutter, K. J.; Fütterman, G.; Wolfrum, J.; Greulich, K. O. *Cytometry* **1991**, *12*, 497–504.
- (2) Battersby, B. J.; Lawrie, G. A.; Johnston, A. P. R.; Trau, M. *Chem. Commun.* **2002**, *14*, 1435–1441.
- (3) Terray, A.; Oakey, J.; Marr, D. W. M. *Science* **2002**, *296*, 1841–1844.
- (4) Gittes, F.; Schnurr, B.; Olmsted, P. D.; MacKintosh, F. C.; Schmidt, C. F. *Phys. Rev. Lett.* **1997**, *79*, 3286–3289.
- (5) Mason, T. G.; Ganesan, K.; van Zanten, J. H.; Wirtz, D.; Kuo, S. C. *Phys. Rev. Lett.* **1997**, *79*, 3282–3285.
- (6) Yamada, S.; Wirtz, D.; Kuo, S. C. *Biophys. J.* **2000**, *78*, 1736–1747.
- (7) Crocker, J. C.; Valentine, M. T.; Weeks, E. R.; Gisler, T.; Kaplan, P. D.; Yodh, A. G.; Weitz, D. A. *Phys. Rev. Lett.* **2000**, *85*, 888–891.
- (8) MacKintosh, F. C.; Schmidt, C. F. *Curr. Opin. Colloid Interface Sci.* **1999**, *4*, 300–307.
- (9) Palmer, A.; Mason, T. G.; Xu, J. Y.; Kuo, S. C.; Wirtz, D. *Biophys. J.* **1999**, *76*, 1063–107.
- (10) Furdul, V. I.; Kariuki, J. K.; Harrison, D. J. *J. Micromech. Microeng.* **2003**, *13*, S164–S170.
- (11) Liu, R. H.; Yang, J. N.; Lenigk, R.; Bonanno, J.; Grodzinski, P. *Anal. Chem.* **2004**, *76*, 1824–1831.
- (12) Lindquist, S. *Ann. Rev. Biochem.* **1986**, *55*, 1151–1191.
- (13) Babincova, M.; Leszczynska, D.; Sourivong, P.; Babinec, P. *Med. Hypotheses* **2000**, *54*, 177–179.
- (14) Hilger, I.; Andra, W.; Hergt, R.; Hiergeist, R.; Schubert, H.; Kaiser, W. A. *Radiology* **2001**, *218*, 570–575.
- (15) Hilger, I.; Frühauf, K.; Andra, W.; Hiergeist, R.; Hergt, R.; Kaiser, W. A. *Acad. Radiology* **2002**, *9*, 198–202.
- (16) Gupta, A. K.; Gupta, M. *Biomaterials* **2005**, *26*, 1565–1573.
- (17) Yellen, B.; Friedman, G.; Feinerman, A. *J. Appl. Phys.* **2003**, *93*, 7331–7333.
- (18) Yellen, B.; Friedman, G.; Feinerman, A. *J. Appl. Phys.* **2002**, *91*, 8552–8554.
- (19) Gunnarsson, K.; Roy, P. E.; Felton, S.; Pihl, J.; Svedlin, P.; Berner, S.; Lidbaum, H.; Oscarsson, S. *Adv. Mater.* **2005**, *17*, 1730–1734.
- (20) Reimann, P.; Hänggi, P. *Appl. Phys. A* **2002**, *75*, 169–178.
- (21) Helseth, L. E.; Backus, T.; Johansen, T. H.; Fischer, T. M. *Langmuir* **2005**, *21*, 7518–7523.
- (22) Garcia, A. A.; Egatz-Gomez, A.; Lindsaya, S. A.; Dominguez-Garcia, P.; Mellea, S.; Marqueza, M.; Rubio, M. A.; Picraux, S. T.; Yang, D.; Aellad, P.; Hayese, M. A.; Gust, D.; Loyprasert, S.; Vazquez-Alvarez, T.; Wang, J. J. *Magn. Magn. Mater.* **2007**, *311*, 238–243.